

# Bilinear $R$ Parity Violation at the ILC – Neutrino Physics at Colliders

J. List<sup>1</sup> and B. Vormwald<sup>1,2</sup>

<sup>1</sup>*Deutsches Elektronen-Synchrotron (DESY),  
Notkestraße 85, D-22607 Hamburg, Germany*

<sup>2</sup>*Universität Hamburg, Inst. f. Exp.-Physik,  
Luruper Chaussee 149, D-22761 Hamburg, Germany*

(Dated: April 4, 2019)

Supersymmetry (SUSY) with bilinearly broken  $R$  parity (bRPV) offers an attractive possibility to explain the origin of neutrino masses and mixings. Thereby neutralinos become a probe to the neutrino sector since studying neutralino decays gives access to neutrino parameters at colliders. We present the study of a bRPV SUSY model at the International Linear Collider (ILC), with the bRPV parameters determined from current neutrino data.

The ILC offers a very clean environment to study the neutralino properties as well as their subsequent decays, which typically involve a  $W/Z$  and a lepton. This study is based on ILC beam parameters according to the Technical Design Report for a center of mass energy of 500 GeV. Full detector simulation of the International Large Detector (ILD) was performed for SUSY and Standard Model processes.

We show for the fully simulated example point that the  $\tilde{\chi}_1^0$  mass can be reconstructed with an uncertainty of less than 0.2% for an integrated luminosity of  $100 \text{ fb}^{-1}$  from direct  $\tilde{\chi}_1^0$  pair production, thus to a large extent independently of the rest of the SUSY spectrum. We also demonstrate that the achievable precision on the atmospheric neutrino mixing angle  $\sin^2 \theta_{23}$  from measuring the neutralino branching fractions  $\text{BR}(\tilde{\chi}_1^0 \rightarrow W\mu)$  and  $\text{BR}(\tilde{\chi}_1^0 \rightarrow W\tau)$  at the ILC is comparable to current uncertainties from neutrino experiments. Thus the ILC could have the opportunity to unveil the mechanism of neutrino mass generation.

## I. INTRODUCTION

Supersymmetry (SUSY) [1, 2] is a very appealing extension of the Standard Model (SM). It gives an elegant solution to the Higgs hierarchy problem, makes gauge unification possible and apart from that, SUSY is the only non-trivial extension of the Lorentz algebra [3]. In the most general renormalizable Lagrangian of the Minimal Supersymmetric Standard Model (MSSM) trilinear and bilinear terms appear, which break baryon number  $B$  and lepton number  $L$ .

The presence of all these terms would lead to proton decay, which is experimentally not observed. A common way to circumvent this problem is to introduce a discrete  $\mathbb{Z}_2$  symmetry assigned to each field in order to suppress these terms. This quantum number, called  $R$  parity, has the form

$$R = (-1)^{3B+L+2S}, \quad (1.1)$$

where  $B$  is the baryon number,  $L$  the lepton number and  $S$  the spin of the field. Hence, SM particles always carry  $R = +1$  and SUSY particle  $R = -1$ . The conservation of this quantum number has the consequence, that all  $B$  and  $L$  breaking terms in the SUSY Lagrangian are forbidden and the proton remains stable.

However, proton decay only appears if  $B$  and  $L$  violation is present at the same time. So, breaking either  $B$  or  $L$  is well consistent with proton stability. Especially in the neutral lepton sector,  $L$  violation is known to be present manifesting in the observation of neutrino oscillations. Thus,  $R$  parity violating (RPV) SUSY scenarios are also viable alternatives to the widely studied  $R$  parity conserving (RPC) scenarios.

We will focus in the following on bilinear  $R$  parity violation (bRPV), which has the interesting feature to be able to introduce neutrino masses and mixings. This mechanism has already been studied theoretically in detail in the literature ([5–9]).

The superpotential and the corresponding soft SUSY breaking terms in bRPV SUSY has the form

$$W^{\text{MSSM}} = W_{\text{RPC}}^{\text{MSSM}} + \epsilon_i L_i H_u, \quad (1.2)$$

$$\mathcal{L}_{\text{soft}}^{\text{MSSM}} = \mathcal{L}_{\text{soft,RPC}}^{\text{MSSM}} + \epsilon_i B_i L_i H_u, \quad (1.3)$$

where  $i = \{e, \mu, \tau\}$  is the generation index.  $H_u$  indicates the  $SU(2)$  doublet of the Higgs superfield and  $L_i$  the  $SU(2)$  doublet of the lepton superfield.  $\epsilon_i$  and  $B_i$  are bRPV parameters. In addition to that, the three sneutrinos acquire a vacuum expectation value (VEV)  $\langle \tilde{\nu}_i \rangle = v_i$ . Because of three additional tadpole equations one ends up with 6 free parameters for bRPV. These parameters can be fixed by fitting them to neutrino observables, like neutrino mass differences and generation mixings.

The introduction of lepton number violation allows the neutrinos to mix with the other neutral fermions of the model, i.e. the gauginos and higgsinos. Thus, in the basis of neutral fermions  $\Psi^{0T} = (\tilde{B}, \tilde{W}^0, \tilde{H}_d^0, \tilde{H}_u^0, \nu_e, \nu_\mu, \nu_\tau)$  the corresponding mass term in the Lagrangian looks like

$$L = -\frac{1}{2} (\Psi^0)^T \mathbf{M}_N \Psi^0 + c.c., \quad (1.4)$$

where the mass matrix  $\mathbf{M}_N$  has off-diagonal entries due to bilinear  $R$  parity breaking.

Diagonalizing  $\mathbf{M}_N$  generates one neutrino mass at tree level as well as two neutrino mixing angles. The atmospheric neutrino mixing angle, for instance, writes as

$$\tan(\theta_{23}) = \frac{\Lambda_\mu}{\Lambda_\tau}, \quad (1.5)$$

where  $\Lambda_i = \mu v_i + v_d \epsilon_i$  are so called alignment parameters. Herein,  $\mu$  is the MSSM higgsino mass parameter and  $v_d$  represents the VEV of the down-type Higgs. It was show in [8] that the remaining neutrino mixing angle and neutrino masses can be derived on 1-loop level.

A very interesting feature of this model is the fact that one can find the left part of the  $\tilde{\chi}_1^0 - W - l_i$ -coupling to be approximately proportional to the alignment parameters

$$O_{\tilde{\chi}_1^0 W l_i} \simeq \Lambda_i \cdot f(M_1, M_2, \mu, v_d, v_u) \propto \Lambda_i, \quad (1.6)$$

where  $f$  is a function of the soft SUSY breaking parameters. The full expression of  $O_{\tilde{\chi}_1^0 W l_i}$  can be found in [9]. Combining eq. (1.5) with eq. (1.6) makes clear that neutrino mixing can be determined from measuring branching ratios of the neutralino decays:

$$\tan^2(\theta_{23}) \simeq \frac{O_{\tilde{\chi}_1^0 W \mu}^2}{O_{\tilde{\chi}_1^0 W \tau}^2} = \frac{\text{BR}(\tilde{\chi}_1^0 \rightarrow W \mu)}{\text{BR}(\tilde{\chi}_1^0 \rightarrow W \tau)} \quad (1.7)$$

The exact relation only holds at tree level. Ref. [9] shows that from 1-loop calculations of the mass matrix dependencies on additional SUSY parameters enter. This can be addressed by considering an parametric uncertainty on relation (1.7), which is estimated to be in the range of 10 to 30% [9].

It is worth mentioning that for bRPV SUSY there is always a connection between LSP decays and neutrino physics independently of the type of the LSP, which is shown in [10].

The aim of the following analysis is to study the performance of measuring the atmospheric neutrino mixing angle in a bRPV SUSY scenario at the International Linear Collider.

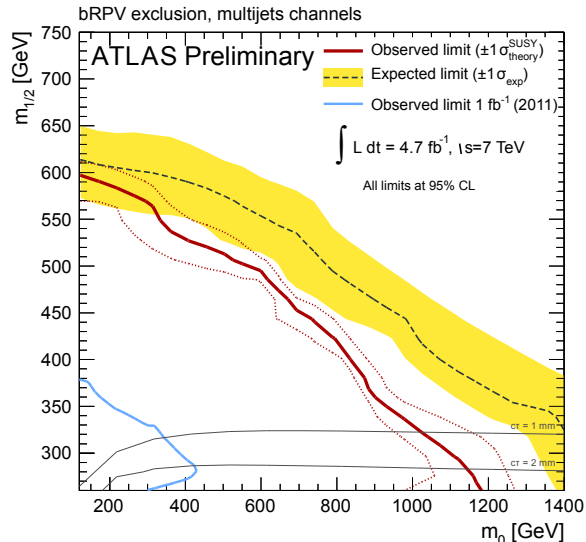


FIG. 1: Expected and observed 95% CL exclusion limits in the bilinear R-parity violating model by the ATLAS experiment. Fig. take from [11].

## II. STATUS AT THE LHC

In pp collisions the dominant SUSY production mode is via squark and gluino production. Those coloured particles then decay via cascades down to the lightest SUSY particle (LSP), which in the RPV case then decays into Standard Model particles. The main difference to RPC studies is that the cut on missing energy is relaxed significantly, since the LSP does not escape undetected anymore.

The ATLAS collaboration performed a dedicated bRPV SUSY search in the framework of the CMSSM, where the RPV parameters were fitted to neutrino data and were not taken as free [11]. In this study contributions from all possible production modes were taken into account. This study excludes a wide range of the CMSSM parameter plane as it is depicted in fig. 1. However, most of the exclusions of the parameter space result from limits on coloured particles for the specific parameter points.

Except for this, various RPV SUSY searches have been performed in the simplified model framework [12–18]. Many of these studies assume strong production, which is dominant for not too high squark or gluino masses. So, the derived limits are predominantly limits on the coloured sector of the model and the electroweak sector remains untested. It could well be that there is a rather large splitting in the SUSY mass spectrum between the electroweak and the coloured sector.

Therefore, it is necessary to search for SUSY also in direct electroweakino production, which has a cross section of some orders of magnitudes below the strong production and, thus, is much more challenging at the LHC. Nevertheless, LHC now starts to become sensitive in the RPC as well as in the RPV case to these production modes and is able to set limits on electroweakino masses [19–22].

However, the cross section for direct  $\tilde{\chi}_1^0 \tilde{\chi}_1^0$  production is well below the sensitivity at the LHC. So, usually a production of a pair of heavier electroweakinos is considered, which decay via the LSP to the Standard Model. Therefore, the limits can only be given as a combination of  $\tilde{\chi}_1^0$  mass and the mass of a heavier electroweakino. In the RPV case, currently one study is present that assumes direct production and one additional non-vanishing trilinear RPV coupling [19]. From

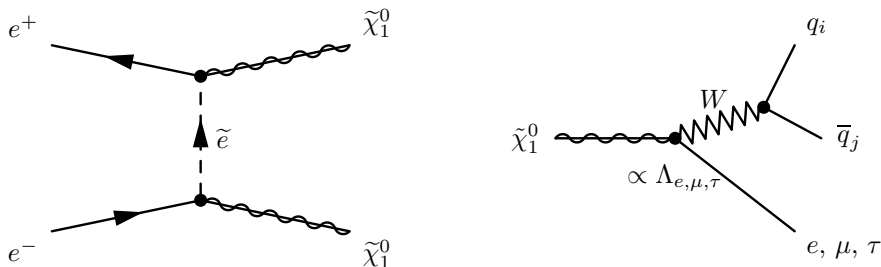


FIG. 2: Left: Main production channel for an bino-like LSP at the ILC: t-channel exchange of an selectron. Right: LSP decay to on-shell  $W$  and a lepton offers direct access to bRPV alignment parameters  $\Lambda_i$  that account for neutrino mixing.

this analysis, limits on  $m_{\tilde{\chi}_1^0}$  can be set for  $m_{\tilde{\chi}_1^\pm} < 750$  GeV. However, one has to note that these limits are very dependent on the assumptions for the type and strength of RPV couplings and it is not directly possible to re-interpret the limits for an bRPV scenario, which accounts for neutrino data.

### III. MODEL DEFINITION

At the ILC the situation is complementary to the LHC: Here, direct electroweakino production is dominant and the electroweak sector can directly be probed.

In our scenario we assume the lightest neutralino being a bino, which leaves only the  $t/u$ -channel production for direct  $\tilde{\chi}_1^0$  pair production (see fig. 2). In presence of bRPV couplings, not only selectrons are possible as exchange particle, but due to the additional terms in principle all other charged scalars could contribute. However, these contributions are strongly suppressed. We define a simplified model in which we set all SUSY particles to a rather high mass except for  $m_{\tilde{\chi}_1^0}$  and  $m_{\tilde{e}_R}$  and, thus those two parameters fix the production cross section.

In the case of a wino LSP, the cross section would drop due to the missing coupling to the right selectron. For a light left selectron, however, the situation is comparable to the bino case. A higgsino-like LSPs would allow  $s$ -channel associate production of  $\tilde{\chi}_1^0$  and  $\tilde{\chi}_2^0$ , predominantly via a  $Z$  boson. In a light higgsino scenario  $\tilde{\chi}_1^0$  and  $\tilde{\chi}_2^0$  are usually close in mass and the decay products of  $\tilde{\chi}_2^0$  to  $\tilde{\chi}_1^0$  are rather soft. Thus, experimentally the situation is comparable to direct  $\tilde{\chi}_1^0$  pair production.

At the ILC up to 80% polarized electron and up to 60% polarized positron beams are possible [23, 24]. In the case of  $t/u$ -channel production with selectron exchange different combinations of beam polarization influence the production cross section significantly. Figure 3 shows the cross-section in the  $\tilde{e}_R$ - $\tilde{\chi}_1^0$  mass plane for unpolarised beams (left) and for the baseline polarisation of  $P(e^+, e^-) = (-30\%, +80\%)$  (right), which enhances the cross-section considerably.

Since the RPV couplings are very small when they are used to describe neutrino data, light LSPs can become rather long-lived with a decay length of meters up to kilometers and escape the detector. Figure 4 (left) shows the decay length of the LSP vs. its mass, while the right-hand panel shows the impact parameter resolution of the ILD detector concept as determined from full detector simulation [25]. For very light LSPs such a scenario would be very hard to determine from RPC SUSY scenarios, but could still be observable in dark matter searches via radiative LSP production [26]. However, in this study we focus on parts of the parameter space, where the on-shell  $W$ -decay channel is available. In this range one expects displaced vertices of the neutralino in the range of a few cm down to 100  $\mu\text{m}$ , which is well detectable.

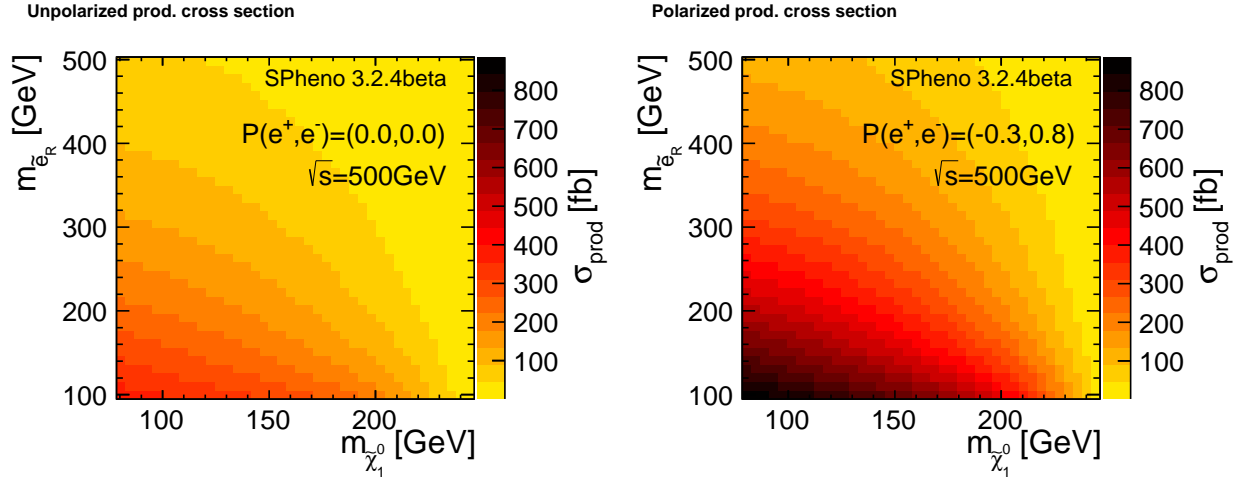


FIG. 3: Unpolarised and polarised production cross section at the ILC500 in the described simplified model. Beam polarization can significantly enhance the production cross section.

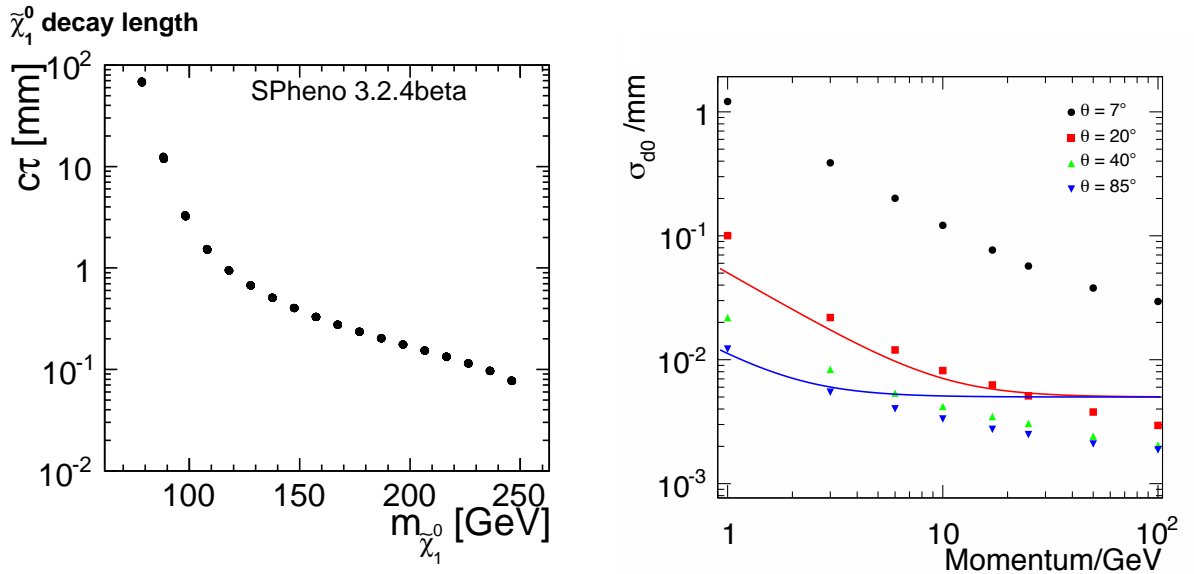


FIG. 4: Left: Decay length of the LSP in dependence of its mass in the simplified model. For a light spectrum of the remaining sparticles, the decay length can be smaller. Right: Impact parameter resolution of the ILD detector concept (from [25]).

For the ILC study the following example point was used:

$$m_{\tilde{\chi}_1^0} = 98.48 \text{ GeV} \quad (3.1)$$

$$m_{\tilde{e}_R} = 280.72 \text{ GeV} \quad (3.2)$$

The mass of the neutralino was selected as a worst case scenario, where  $m_{\tilde{\chi}_1^0} \simeq m_{W/Z}$ . This is most challenging, since in this case the LSP signal is expected to overlay significantly with SM background and the involved leptons from the LSP decay to  $W$  become relatively soft.

The production cross section for the polarization  $\mathcal{P}(e^+, e^-) = (-30\%, +80\%)$  and a center of mass energy of  $\sqrt{s} = 500 \text{ GeV}$  amounts to 384 fb, driven by the choice of  $m_{\tilde{e}_R}$ . As can be seen from figure 3, the production cross section is still  $\sim 100 \text{ fb}$  when  $m_{\tilde{e}_R}$  is twice as large. The branching

ratios for the decay modes that are relevant for measuring the neutrino atmospheric mixing angle (see eq. (1.7)) read  $BR(\tilde{\chi}_1^0 \rightarrow \mu^\pm W^\mp) = 0.30$  and  $BR(\tilde{\chi}_1^0 \rightarrow \tau^\pm W^\mp) = 0.27$ . The remaining fraction comes mainly from on-shell  $Z$  decay modes  $\tilde{\chi}_1^0 \rightarrow \nu_i Z$  and three-body decays. For an integrated luminosity of  $100 \text{ fb}^{-1}$  one expects 38400 produced neutralino pairs and among them 3456 events ending up in the  $\mu\mu$ -channel, 2799 events in the  $\tau\tau$ -channel and 6221 events in the mixed  $\mu\tau$ -channel. As the ILC is expected to deliver an integrated luminosity of  $250 \text{ fb}^{-1}/\text{year}$ , this amount of data is going to be collected within approximately five months of operation at design luminosity.

#### IV. DATA SAMPLES

For the given example point a full detector simulation of the International Large Detector (ILD) [25] for an integrated luminosity of  $100 \text{ fb}^{-1}$  and a center of mass energy of  $\sqrt{s} = 500 \text{ GeV}$  was performed. For the SM background, samples produced for the benchmarking of the ILD detector for the Technical Design Report have been used.

In the case of bRPV events the program `Sarah` [28] was used to generate model files for the event generator. As for the SM samples, `Whizard` [29] was used as event generator of the hard process and `Pythia` [30] for fragmentation and hadronization. These events were passed through `Mokka` [31], the full `Geant4`-based [32] simulation of the ILD detector and finally reconstructed with `MarlinReco` [33]. For the event generation realistic beam parameters were taken into account, including the ILC specific beam energy spectrum at 500 GeV.

With the instantaneous luminosity foreseen at the ILC, on average 1.7 interactions of photons leading to the production of low  $p_t$  hadrons are expected per bunch-crossing. This takes into account contributions from real photons accompanying the electron beam due to bremsstrahlung and synchrotron radiation as well as from virtual photons radiated off the primary beam electrons. Therefore, each hard-interaction event (from SUSY or SM background) was overlaid with a randomly chosen number of such  $\gamma\gamma \rightarrow$  hadrons events before the reconstruction step.

#### V. EVENT SELECTION

The signal events have a rather clear signature: The produced LSPs decay into either a  $\mu$  or  $\tau$  plus a  $W$  boson. In the following we restrict ourselves to the hadronic  $W$  decay mode. Thereby, the event is – except for some missing energy from a potential  $\tau$  decay – fully reconstructable with 6 visible fermions in the final state.

Before the actual event selection is performed, the  $\gamma\gamma \rightarrow$  hadrons background is removed from the event by the following procedure: Since we expect to have six final states, an exclusive  $k_T$  jet clustering algorithm ( $R = 1.3$ ) which is forced to find six jets is applied to the reconstructed objects in the events. This algorithm builds up six jets which are assigned to the hard interaction and in addition to them two very forward directed beam jets which are treated as beam background. Removing those beam jets and using only the objects which end up clustered in the main jets for the further analysis, recovers very well the bare event without background overlay. Fig. 5 shows the impact of overlaid  $\gamma\gamma$  events on the visible energy (left) and the ability to remove this background with the described method (right).

Two hadronically decaying  $W$ s imply a relatively high particle multiplicity  $N_{\text{objects}}$  in the event. And due to the fact, that there is no major source for missing energy, the visible energy in the

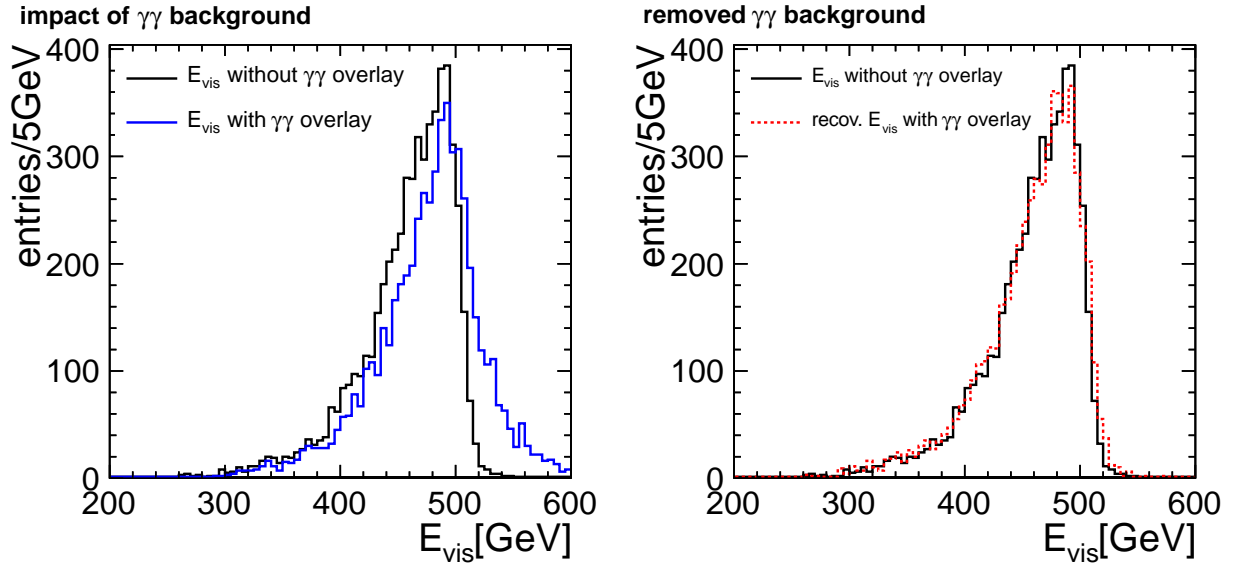


FIG. 5: Left: Effect of  $\gamma\gamma \rightarrow$  hadrons background overlay to visible energy of the event. Right: Recovered visible energy in the event after  $\gamma\gamma \rightarrow$  hadrons background removal procedure.

event is rather high. So, the following preselection cuts were used:

$$E_{\text{visible}} \geq 350 \text{ GeV} \quad (5.1)$$

$$50 \geq N_{\text{objects}} \geq 150, \quad (5.2)$$

This preselection on the one hand reduces Standard Model background and on the other hand cuts away some of the leptonic  $W$  contribution in the LSP decay, which is not considered as signal in this analysis. The preselection signal efficiency finally amounts to 95%.

In order to be able to measure the ratio of different branching ratios of the LSP decay (see eq. (1.7)) we have to define a selection to distinguish between the different event classes:

**$\mu\mu$  class** Here we look for an event with at least two reconstructed muons. The two most energetic ones are removed from the event. No further lepton isolation criteria is required. The remaining objects of the event are clustered by the Durham jets clustering algorithm into four jets. All permutations of the four jets are tried to combine them into two  $W$ s. The quantity

$$\chi_{W_i}^2 = \left( \frac{m_{\text{reco},i} - m_W}{\sigma_{\text{res}}} \right)^2 \quad (5.3)$$

is used to find the best combination of objects to form  $W$  candidates, by finding the minimal possible value. The factor  $\sigma_{\text{res}} = 5 \text{ GeV}$  is an assumed resolution factor. All combinations of  $W$  candidates and muons are then used to try to reconstruct two equal mass objects. Those two objects with the smallest

$$\chi_{\text{eqm}}^2 = \left( \frac{m_{\text{reco},1} - m_{\text{reco},2}}{\sigma_{\text{res}}} \right)^2 \quad (5.4)$$

are considered as LSP candidates. If the event fulfills the condition

$$\chi_{W_1}^2 < 2 \quad \text{and} \quad \chi_{W_2}^2 < 2 \quad \text{and} \quad \chi_{\text{eqm}}^2 < 2, \quad (5.5)$$

the event is counted as  $\mu\mu$  event, else it is tested against the  $\mu\tau$  class.

**$\mu\tau$  class** In this class at least one reconstructed muon in the event is required. The most energetic muon is removed and the rest of the event is forced into five jets by an inclusive Durham jet clustering algorithm. Since the muon requirement is relaxed, one expects to be more prone to select background events. For this reason we test in addition, whether this jet configuration describes the event well. Therefore, we employ a cut on the Durham jet algorithm parameters  $y_{i-1,i}$  and  $y_{i,i+1}$ . Hereby, the parameter  $y_{i-1,i}$  is a measure of the distance in energy-momentum space between two of the  $i$  jets which would be merged, if a  $i - 1$  configuration was required. The second parameter  $y_{i,i+1}$ , however, gives the same measure when requiring an  $i + 1$  configuration for the same event with respect to the original  $i$  configuration. For a well describing five jet configuration,  $y_{4,5} - y_{5,6}$  gets maximal, so we use the following cut:

$$y_{4,5} - y_{5,6} > 0.5 \cdot 10^{-4}. \quad (5.6)$$

The jet with the least constituents is considered as tau candidate and removed from the event, if  $N_{\text{const.}} < 10$ . Additionally it is required that the jet does not contain a muon. The further approach to find  $W$  candidates and finally LSP candidates is identical to the  $\mu\mu$  class. If condition (5.5) is satisfied this event is counted as  $\mu\tau$  event, otherwise the  $\tau\tau$  class is tested.

**$\tau\tau$  class** The event is forced into six jets by an inclusive Durham jet clustering algorithm. In analogy to the  $\mu\tau$  class, it is required that  $y_{5,6} - y_{6,7} > 0.5 \cdot 10^{-4}$ . The two jets with the least constituents are considered as tau candidates and removed from the event, if both candidates fulfill  $N_{\text{const.}} < 10$  and a muon-veto. The further approach to find  $W$  candidates and finally LSP candidates is identical to the  $\mu\mu$  and  $\mu\tau$  class. If condition (5.5) is satisfied this event is counted as  $\tau\tau$  event.

After this selection fig. 6 shows the reconstructed neutralino mass in each of the event classes. The main remaining background comes from  $WW$  and  $ZZ$  pairs, which can to some extent fulfill the described selection criteria.

The  $\mu\mu$  class has a very clear signal peak, which can be used for measuring the LSP mass. After SM background subtraction and a fit of a Gaussian to the the distribution we get:

$$m_{\tilde{\chi}_1^0}^{\text{fit}} = 98.39 \pm 0.13(\text{stat.}) \quad (5.7)$$

The measured value is within the error in very good agreement with the input mass of the example point (see eq. (3.1)).

This precision measurement of the LSP mass in the  $\mu\mu$  channel can now be used to define a signal region  $m_{\tilde{\chi}_1^0}^{\text{fit}} \pm 10$  GeV. This further reduces the background fraction in the selected event classes. The decomposition of number of measured events in the different event classes  $N^{\text{reco}}$  into the number of events in the different truth classes  $N^{\text{true}}$  is shown in the the following matrix  $\mathbf{N}$ :

$$\mathbf{N} = \begin{matrix} & N_{\mu\mu}^{\text{true}} & N_{\mu\tau}^{\text{true}} & N_{\tau\tau}^{\text{true}} & N_{\text{LSPBG}}^{\text{true}} & N_{\text{SMBG}}^{\text{true}} \\ \begin{matrix} N_{\mu\mu}^{\text{reco}} \\ N_{\mu\tau}^{\text{reco}} \\ N_{\tau\tau}^{\text{reco}} \end{matrix} & \begin{pmatrix} 482 & 77 & 4 & 40 & 69 \\ 9 & 183 & 16 & 15 & 66 \\ 0 & 1 & 38 & 4 & 59 \end{pmatrix} \end{matrix} \quad (5.8)$$

Thereby  $N_{\text{LSPBG}}^{\text{true}}$  denotes those events, in which at least one LSP decays differently than the aimed two-body decay  $\tilde{\chi}_1^0 \rightarrow Wl$ .

The signal over background ratio in the different classes becomes:



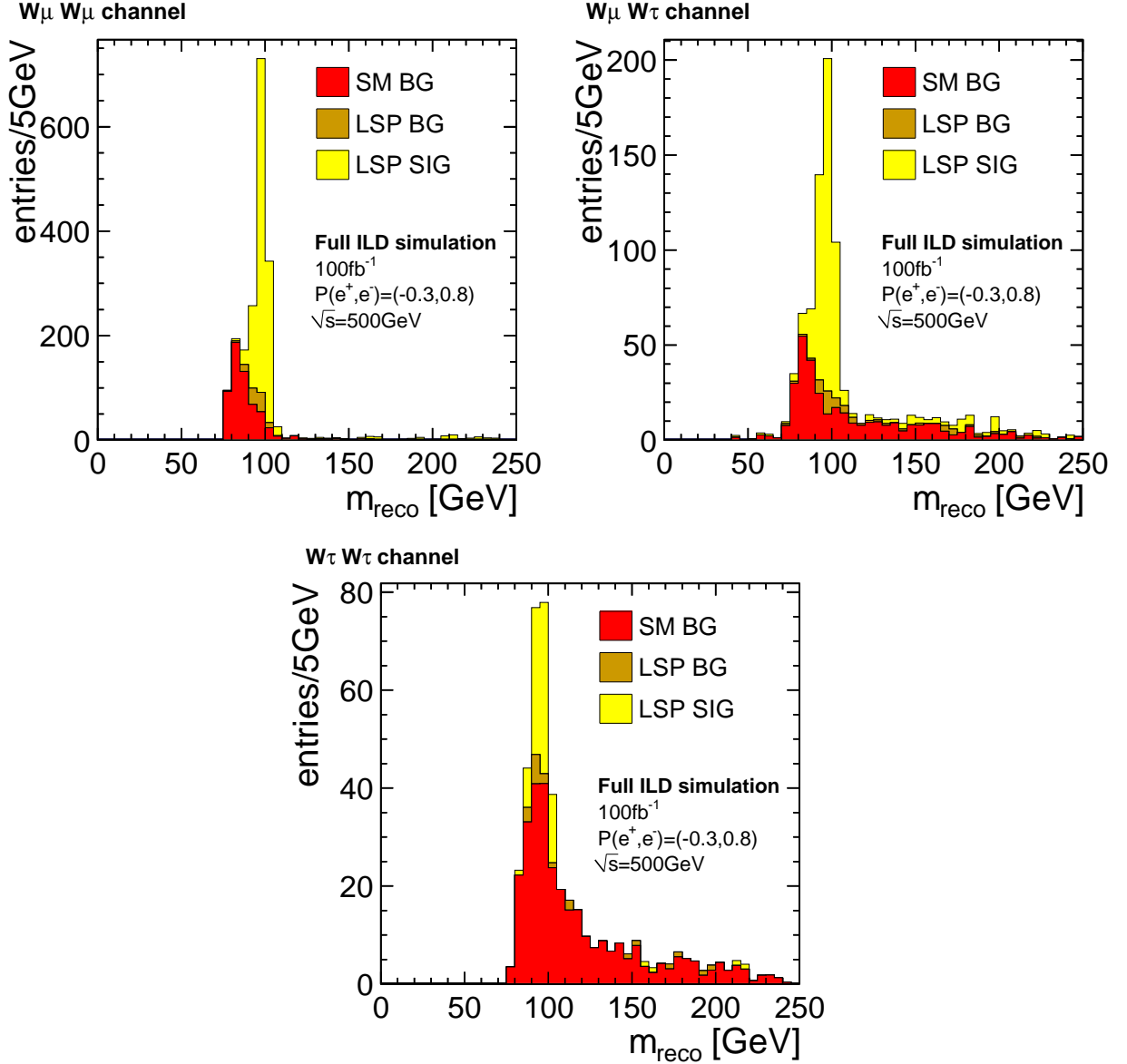


FIG. 6: Mass reconstruction of the LSP for the different event classes with full Standard Model background included.

	$S/\sqrt{B}$
$\mu\mu$ class	53.9
$\mu\tau$ class	23.1
$\tau\tau$ class	4.9

As expected the  $\tau\tau$  channel is by far the one with the lowest purity. However, for measuring the ratio of branching ratios this channel is not needed, as it will be discussed in the next section.

It was already pointed out that this studied parameter point is a worst case scenario. It is clearly visible in fig. 6 that for another parameter point with a higher LSP mass the signal peak would shift into an almost completely background-free region. Though, the LSPs in this model become rather long-lived in the Standard Model polluted, “low-mass” region (compare fig. 4). Adding this information to the analysis and requiring from the reconstructed objects not to point to the

primary vertex, would reduce the Standard Model background drastically. However, this would on the other hand introduce a strong model dependency to the analysis. Therefore the exploitation of the lifetime information is left as a future option for improvements.

## VI. BRANCHING RATIO MEASUREMENT AND NEUTRINO INTERPRETATION

We assume in the following that the Standard Model background can be estimated from Monte Carlo accurately and can be subtracted. Also the LSP non-signal decays can be predicted to some extent, as soon as one has some additional knowledge about the remaining SUSY mass spectrum. Under this assumption we can build a  $3 \times 3$  efficiency matrix  $\mathbf{E}$ , which is defined like

$$(\mathbf{E})_{ij} = \frac{(N)_{ij}}{N_i^{\text{true}}} = \begin{pmatrix} \mathbf{0.3088} & 0.0290 & 0.0034 \\ 0.0058 & \mathbf{0.084} & 0.0136 \\ 0.0000 & 0.0004 & \mathbf{0.0324} \end{pmatrix}_{ij}. \quad (6.1)$$

The vector of measured events becomes

$$\vec{N}^{\text{reco}} = \begin{pmatrix} N_{\mu\mu}^{\text{reco}} - N_{BG,\mu\mu}^{\text{MC}} \\ N_{\mu\tau}^{\text{reco}} - N_{BG,\mu\tau}^{\text{MC}} \\ N_{\tau\tau}^{\text{reco}} - N_{BG,\tau\tau}^{\text{MC}} \end{pmatrix}, \quad \Delta \vec{N}^{\text{reco}} = \begin{pmatrix} \sqrt{N_{\mu\mu}^{\text{reco}} + N_{BG,\mu\mu}^{\text{MC}}} \\ \sqrt{N_{\mu\tau}^{\text{reco}} + N_{BG,\mu\tau}^{\text{MC}}} \\ \sqrt{N_{\tau\tau}^{\text{reco}} + N_{BG,\tau\tau}^{\text{MC}}} \end{pmatrix}. \quad (6.2)$$

The efficiency matrix can then be inverted and used to calculate the true number of events in the different event classes.

$$\vec{N}^{\text{true}} = \mathbf{E}^{-1} \vec{N}^{\text{reco}} \quad (6.3)$$

The ratio of the two branching ratios can be extracted in different ways:

$$\frac{\text{BR}(\tilde{\chi}_1^0 \rightarrow W\mu)}{\text{BR}(\tilde{\chi}_1^0 \rightarrow W\tau)} = \frac{2N_{\mu\mu}^{\text{true}}}{N_{\mu\tau}^{\text{true}}} = \frac{N_{\mu\tau}^{\text{true}}}{2N_{\tau\tau}^{\text{true}}} = \sqrt{\frac{N_{\mu\mu}^{\text{true}}}{N_{\tau\tau}^{\text{true}}}}, \quad (6.4)$$

since for the expected true number of events the following relations hold:

$$N_{\mu\mu}^{\text{true}} = N_{\tilde{\chi}_1^0 \tilde{\chi}_1^0} \cdot \text{BR}^2(\tilde{\chi}_1^0 \rightarrow W\mu) \quad (6.5)$$

$$N_{\mu\tau}^{\text{true}} = N_{\tilde{\chi}_1^0 \tilde{\chi}_1^0} \cdot 2 \cdot \text{BR}(\tilde{\chi}_1^0 \rightarrow W\mu) \cdot \text{BR}(\tilde{\chi}_1^0 \rightarrow W\tau) \quad (6.6)$$

$$N_{\tau\tau}^{\text{true}} = N_{\tilde{\chi}_1^0 \tilde{\chi}_1^0} \cdot \text{BR}^2(\tilde{\chi}_1^0 \rightarrow W\tau) \quad (6.7)$$

where  $N_{\tilde{\chi}_1^0 \tilde{\chi}_1^0} = \sigma(e^+e^- \rightarrow \tilde{\chi}_1^0 \tilde{\chi}_1^0) \cdot \int \mathcal{L} dt$  is the number of produced LSP pairs. Because of the low selection purity in the  $\tau\tau$  channel, we have chosen the relation involving only the  $\mu\mu$  and  $\mu\tau$  channel.

In order to estimate the statistical uncertainty on the resulting ratio of event numbers, an error propagation was performed, assuming binomial error in the efficiency matrix and Poissonian errors for the reconstructed number of events.

The resulting statistical uncertainty is depicted in fig. 7 in dependence of integrated luminosity at the ILC500. For the studied parameter point the achievable precision for  $\int \mathcal{L} dt = 100 \text{ fb}^{-1}$  is about 14%. This scales down to roughly 6% for  $500 \text{ fb}^{-1}$ , which is the desired integrated luminosity at ILC500 in a first stage.

The measured ratio of branching ratios can now be translated into the atmospheric mixing angle following eq. (1.7). As discussed earlier, the given relation is only an approximation and there are

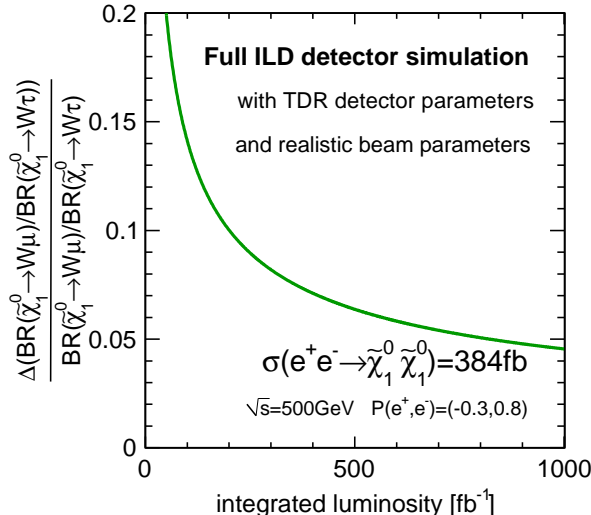


FIG. 7: Achievable measurement precision of the ratio of the muonic and tauonic 2BD decay modes of the LSP at the ILC.

additional parametric uncertainties coming from residual SUSY parameter dependencies [9]. For this reason we define two scenarios in which we add a parametric uncertainty of 10% and 30% to the given relation. From a random SUSY parameter scan performed in [9] it is evident, that 30% is a rather conservative value.

The derived precision of the measurement of the atmospheric neutrino mixing angle for different assumed parametric uncertainties is shown in fig. 8 (left). One can now compare this precision with the uncertainty of current neutrino experiments [34], which is done in fig. 8 (right). The middle red line indicates the best fit value of the atmospheric neutrino mixing angle and the upper and lower dashed red lines indicate the  $1\sigma$  uncertainty. The overlaid precision estimation at the ILC shows, that the ILC can test if neutrino mixing and mass generation is introduced by RPV.

## VII. CONCLUSIONS

We have presented a full ILD detector simulation of a bRPV SUSY model, which is an attractive possibility to explain neutrino mass generation and mixing. A highly detailed ILD model as well as realistic ILC beam parameters were taken into account for the simulation. As studied parameter point, a worst case scenario was used, where  $m_{\tilde{\chi}_1^0} \simeq m_{W/Z}$  and, thus, the signal significantly overlaps with SM background.

We have developed a model independent selection strategy to disentangle the different event classes involving the two decay modes of the LSP  $\tilde{\chi}_1^0 \rightarrow \mu^\pm W^\mp$  and  $\tilde{\chi}_1^0 \rightarrow \tau^\pm W^\mp$ . It has been demonstrated that in the  $\mu\mu$  event class a very accurate mass measurement with an uncertainty of  $\delta m_{\tilde{\chi}_1^0} = 0.13$  GeV is possible for an integrated luminosity of  $100 \text{ fb}^{-1}$ . With the described selection a signal to background ratio of 53.9 in the  $\mu\mu$  event class and 23.1 in the  $\mu\tau$  event class was achieved.

Those two classes have then been used to determine the ratio of the two branching ratios  $\text{BR}(\tilde{\chi}_1^0 \rightarrow \mu^\pm W^\mp) / \text{BR}(\tilde{\chi}_1^0 \rightarrow \tau^\pm W^\mp)$ , which is related to the atmospheric neutrino mixing angle  $\sin^2 \theta_{23}$ . For an integrated luminosity of  $500 \text{ fb}^{-1}$  the statistical uncertainty on this ratio has been determined to 6%.

Finally, we have shown that the precision in measuring the atmospheric neutrino mixing angle

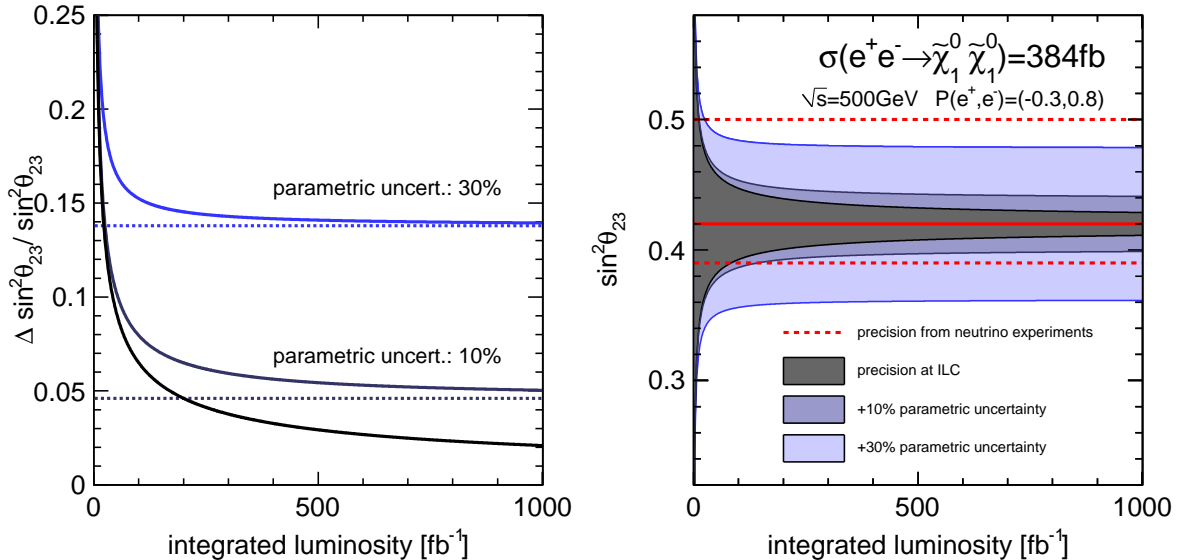


FIG. 8: Precision of the measurement of the atmospheric mixing angle at the ILC. Left: Relative uncertainty assuming different parametric uncertainties on the relation between ratio of branching ratios and atmospheric neutrino mixing angle. Right: Comparison of achievable precision at the ILC with precision at current neutrino experiments.

is comparable to measurements from neutrino oscillation experiments. Therefore, the International Linear Collider is highly capable to test bRPV SUSY as origin of neutrino masses and mixings.

### Acknowledgements

We would like to thank the ILC Generators group and the ILD MC production team for providing the SM background samples. We thank Werner Porod for helpful discussions and for providing the neutrino data fit for the simplified model approach. We thankfully acknowledge the support by the DFG through the SFB 676 ‘‘Particles, Strings and the Early Universe’’.

- 
- [1] J. Wess and B. Zumino, Nucl. Phys. B **70** (1974) 39.
  - [2] J. Wess and B. Zumino, Phys. Lett. B **49** (1974) 52.
  - [3] R. Haag, J. T. Lopuszanski and M. Sohnius, *All Possible Generators of Supersymmetries of the  $s$  Matrix*, Nucl. Phys. B **88** (1975) 257.
  - [4] G. R. Farrar and P. Fayet, *Phenomenology of the Production, Decay, and Detection of New Hadronic States Associated with Supersymmetry*, Phys. Lett. B **76** (1978) 575.
  - [5] J. C. Romao and J. W. F. Valle, *Neutrino masses in supersymmetry with spontaneously broken  $R$  parity*, Nucl. Phys. B **381** (1992) 87.
  - [6] B. Mukhopadhyaya, S. Roy and F. Vissani, *Correlation between neutrino oscillations and collider signals of supersymmetry in an  $R$ -parity violating model*, Phys. Lett. B **443** (1998) 191 [hep-ph/9808265].
  - [7] S. Y. Choi, E. J. Chun, S. K. Kang and J. S. Lee, *Neutrino oscillations and  $R$ -parity violating collider signals*, Phys. Rev. D **60** (1999) 075002 [hep-ph/9903465].
  - [8] M. Hirsch, M. A. Diaz, W. Porod, J. C. Romao and J. W. F. Valle, *Neutrino masses and mixings from supersymmetry with bilinear  $R$  parity violation: A Theory for solar and atmospheric neutrino oscillations*, Phys. Rev. D **62** (2000) 113008 [Erratum-ibid. D **65** (2002) 119901] [hep-ph/0004115].

- [9] W. Porod, M. Hirsch, J. Romao and J. W. F. Valle, *Testing neutrino mixing at future collider experiments*, Phys. Rev. D **63** (2001) 115004 [hep-ph/0011248].
- [10] M. Hirsch and W. Porod, *Neutrino properties and the decay of the lightest supersymmetric particle*, Phys. Rev. D **68** (2003) 115007 [hep-ph/0307364].
- [11] [ATLAS Collaboration], *Search for supersymmetry at  $\sqrt{s} = 7$  TeV in final states with large jet multiplicity, missing transverse momentum and one isolated lepton with the ATLAS detector*, ATLAS-CONF-2012-140.
- [12] [ATLAS Collaboration], *Search for strongly produced superpartners in final states with two same sign leptons with the ATLAS detector using 21 fb<sup>-1</sup> of proton-proton collisions at  $\sqrt{s}=8$  TeV.*, ATLAS-CONF-2013-007.
- [13] G. Aad *et al.* [ATLAS Collaboration], *Search for a heavy narrow resonance decaying to  $e\mu$ ,  $e\tau$ , or  $\mu\tau$  with the ATLAS detector in  $\sqrt{s} = 7$  TeV pp collisions at the LHC*, arXiv:1212.1272 [hep-ex].
- [14] G. Aad *et al.* [ATLAS Collaboration], *Search for pair production of massive particles decaying into three quarks with the ATLAS detector in  $\sqrt{s} = 7$  TeV pp collisions at the LHC*, JHEP **1212** (2012) 086 [arXiv:1210.4813 [hep-ex]].
- [15] [CMS Collaboration], *Search for RPV SUSY resonant second generation slepton production in same-sign dimuon events at  $\sqrt{s} = 7$  TeV*, CMS-PAS-SUS-13-005.
- [16] [CMS Collaboration], *Search for RPV supersymmetry with three or more leptons and b-tags*, CMS-PAS-SUS-12-027.
- [17] [CMS Collaboration], *Search for light stop RPV supersymmetry with three or more leptons and b-tags*, CMS-PAS-SUS-13-003.
- [18] [CMS Collaboration], *Search for RPV SUSY in the four-lepton final state*, CMS-PAS-SUS-13-010.
- [19] [ATLAS Collaboration], *Search for supersymmetry in events with four or more leptons in 21 fb<sup>-1</sup> of pp collisions at  $\sqrt{s} = 8$  TeV with the ATLAS detector*, ATLAS-CONF-2013-036.
- [20] [CMS Collaboration], *Search for direct EWK production of SUSY particles in multilepton modes with 8TeV data*, CMS-PAS-SUS-12-022.
- [21] [ATLAS Collaboration], *Search for direct production of charginos and neutralinos in events with three leptons and missing transverse momentum in 21 fb<sup>-1</sup> of pp collisions at  $\sqrt{s} = 8$  TeV with the ATLAS detector*, ATLAS-CONF-2013-035.
- [22] [ATLAS Collaboration], *Search for electroweak production of supersymmetric particles in final states with at least two hadronically decaying taus and missing transverse momentum with the ATLAS detector in proton-proton collisions at  $\sqrt{s} = 8$  TeV*, ATLAS-CONF-2013-028.
- [23] G. Moortgat-Pick, T. Abe, G. Alexander, B. Ananthanarayan, A. A. Babich, V. Bharadwaj, D. Barber and A. Bartl *et al.*, Phys. Rept. **460** (2008) 131 [hep-ph/0507011].
- [24] C. Adolphsen, M. Barone, B. Barish, K. Buesser, P. Burrows, J. Carwardine, J. Clark and Hln. M. Durand *et al.*, “The International Linear Collider Technical Design Report - Volume 3.II: Accelerator Baseline Design,” arXiv:1306.6328 [physics.acc-ph].
- [25] T. Behnke, J. E. Brau, P. N. Burrows, J. Fuster, M. Peskin, M. Stanitzki, Y. Sugimoto and S. Yamada *et al.*, “The International Linear Collider Technical Design Report - Volume 4: Detectors,” arXiv:1306.6329 [physics.ins-det].
- [26] C. Bartels, M. Berggren and J. List, *Characterising WIMPs at a future  $e^+e^-$  Linear Collider*, Eur. Phys. J. C **72** (2012) 2213 [arXiv:1206.6639 [hep-ex]].
- [27] T. Abe *et al.* [ILD Concept Group - Linear Collider Collaboration], *The International Large Detector: Letter of Intent*, arXiv:1006.3396 [hep-ex].
- [28] F. Staub, *From Superpotential to Model Files for FeynArts and CalcHep/CompHep*, Comput. Phys. Commun. **181** (2010) 1077 [arXiv:0909.2863 [hep-ph]].
- [29] W. Kilian, T. Ohl and J. Reuter, *WHIZARD: Simulating Multi-Particle Processes at LHC and ILC*, Eur. Phys. J. C **71** (2011) 1742 [arXiv:0708.4233 [hep-ph]].  
M. Moretti, T. Ohl and J. Reuter, *O’Mega: An Optimizing matrix element generator*, In \*2nd ECFA/DESY Study 1998-2001\* 1981-2009 [hep-ph/0102195].
- [30] T. Sjostrand, S. Mrenna and P. Z. Skands, *PYTHIA 6.4 Physics and Manual*, JHEP **0605** (2006) 026 [hep-ph/0603175].
- [31] P. Mora de Freitas and H. Videau, “Detector simulation with MOKKA / GEANT4: Present and future,” LC-TOOL-2003-010.
- [32] S. Agostinelli *et al.* [GEANT4 Collaboration], *GEANT4: A Simulation toolkit*, Nucl. Instrum. Meth.

A **506** (2003) 250.

J. Allison, K. Amako, J. Apostolakis, H. Araujo, P. A. Dubois, M. Asai, G. Barrand and R. Capra *et al.*, *Geant4 developments and applications*, IEEE Trans. Nucl. Sci. **53** (2006) 270.

[33] O. Wendt & al., Pramana **69**, (2007) 1109, [physics/0702171].

[34] J. Beringer et al. [Particle Data Group], Phys. Rev. **D86**, 010001 (2012)